MRS Advances (2023) 8:855–859
https://doi.org/10.1557/s43580-023-00642-x

ORIGINAL PAPER

Predicting and understanding corrosion in molten chloride salts

Kerry Rippy[2,3] · Liam Witteman[1,2] · Patrick R. Taylor[3] · Judith C. Vidal[2,3]

Received: 15 June 2023 / Accepted: 5 September 2023 / Published online: 25 September 2023

Abstract
Molten chloride salts are stable at higher temperatures than many other salts, including nitrate salts, and are thus promising for heat transfer and/or thermal energy storage in concentrating solar power, nuclear power, and other thermal energy storage applications. However, corrosion in molten chloride salts remains a significant problem. While many studies have been devoted to evaluation of corrosion, we find that a comprehensive method for predicting corrosion in molten chloride salts is lacking. Here, we present an evaluation of corrosion in molten chloride salts using Ellingham diagrams and chloride-oxide stability diagrams, which enable prediction of alloy performance in molten chloride salts and allow corrosion results to be interpreted at a fundamental level.

Introduction

A comprehensive body of literature exists on the study of corrosion of alloys in molten chlorides [1–19], The focus of corrosion studies has been primarily concerned with Fe-based and Ni-based alloys, i.e., stainless steels versus nickel super alloys. These studies often experimentally evaluate depletion of individual elements in super alloys. However, Ellingham diagrams, often overlooked in the literature, are a useful tool for predicting behavior of alloying elements. In combination with chloride-oxide stability diagrams, Ellingham diagrams can explain much of the experimentally observed behavior of alloys is chloride salts. Typically, super alloys exhibit high corrosion resistance due to the presence of a passivating oxide layer such as chromium oxide. However, in molten chloride salts Cl^- ions challenge this oxide layer, and expose the alloying constituents to further oxidation, creating what has been termed the "chlorine-oxidation cycle" [1–10], For all alloys corrosion follows the same stages of (1) oxidation of elements in alloy, followed by (2) dissolution or vaporization of oxidized elements. The rate of corrosion has therefore been strongly correlated to the presence of oxidizing impurities in the chloride salt [3, 5–11, 13–16, 18–23]. Understanding these studies using Ellingham diagrams and chloride-oxide stability diagrams enables predictive insight into alloy performance. Furthermore, it underscores the importance of limiting corrosive impurities via control of salt exposure to water, oxygen, and other oxidizing agents.

Results and discussion

Construction of Ellingham diagrams

The utility of Ellingham diagrams in evaluating molten chloride salts systems can be illustrated in the example case of $MgCl_2$. The formation of corrosive impurities primarily stem from the hygroscopic nature of $MgCl_2$ resulting in the formation of oxide/hydroxide species in the presence of oxygen and moisture via the following reactions:

$$MgCl_{2(l)} + H_2O_{(g)} \leftrightarrow MgOHCl_{(l)} + HCl_{(g)} \quad (1)$$

$$O_{2(g)} + 4Cl^-_{(l)} \leftrightarrow 2O^{2-}_{(l)} + 2Cl_{2(g)} \quad (2)$$

Furthermore, MgOHCl has been found to decompose above 550°C according

Kerry Rippy and Liam Witteman have contributed equally to this work.

✉ Kerry Rippy
kerry.rippy@nrel.gov

1 Advanced Energy Systems Program, Colorado School of Mines, Colorado, USA

2 National Renewable Energy Laboratory, Colorado, USA

3 Kroll Institute for Extractive Metallurgy, Colorado School of Mines, Colorado, USA

$$MgOHCl_{(l)} \leftrightarrow MgO_{(l)} + HCl_{(g)} \quad (3)$$

nb

Several studies have found a direct correlation between corrosion rates and concentration of MgOHCl present in the chloride salt [20, 23], Furthermore, the formation of $HCl_{(g)}$ and $Cl_{2(g)}$ via leads to corrosion of alloys in the headspace [7, 23, 24]. The corrosive impurities lead to degradation reactions with alloying constituents M (e.g., Cr, Fe, Ni) according to:

$$xHCl_{(g)} + M \leftrightarrow MCl_x + 1/2xH_{2(g)} \quad (4)$$

$$xMgOHCl_{(l)} + M \leftrightarrow xMgO_{(l)} + MCl_x + 1/2xH_{2(g)} \quad (5)$$

$$1/2xO_{2(g)} + yM \leftrightarrow M_yO_x \quad (6)$$

This degradation is an electrochemical process that can be explained via half-cell reactions as follows [9, 25]:

Anodic oxidation of alloying element M:

$$M \rightarrow M^{n+} + ne^- \quad (7)$$

where n is the number of electrons exchanged.

Cathodic reduction of corrosive species:

$$ox + ne^- \rightarrow red \quad (8)$$

where Ox is the oxidizing impurity in this case (e.g. MgOHCl), and Red is the reduced form of the oxidizing impurity.

The complete redox couple reaction:

$$M + ox \longleftrightarrow M^{n+} + red \quad (9)$$

For the electrochemical process to occur spontaneously the change in Gibbs-free energy needs to be negative, which can be calculated via:

$$\Delta G_{rxn} = -nF\Delta E_{rxn} \quad (10)$$

where ΔG_{rxn} is the change in Gibbs-free energy of reaction ($J\ mol^{-1}$), F is Faraday's constant (96,485 C mol^{-1}), and ΔE_{rxn} is the redox potential of reaction (V).

Equation 10 allows for the construction of an Ellingham diagram, shown in Figure 1 (constructed for various alloying constituents using the thermodynamic software HSC v8).

According to Figure 1, the most stable chlorides are K, Na, and Mg. Therefore, common alloying constituents (e.g. Fe, Cr, Ni) should theoretically remain stable within the chloride salt. However, the influence of oxidizing impurities such as MgOHCl is not readily captured by simply looking at Equation 10. To assess the effect of oxidizing impurities, ΔE_{rxn} can be further expressed into the anodic and cathodic potentials via the Nernst Equation:

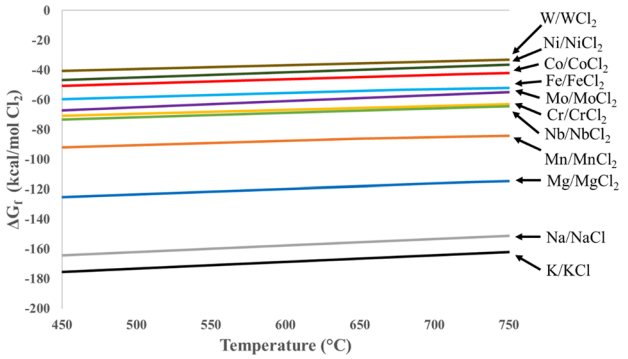

Fig. 1 Gibbs-free energy of reaction of metal to metal-chloride as a function of temperature

$$\Delta E_{rxn} = E_c - E_a \quad (11)$$

$$E_a = E_a^0 + \frac{RT}{nF}\ln\left(\frac{a_{M^{n+}}}{a_M}\right) \quad (12)$$

$$E_c = E_c^0 + \frac{RT}{nF}\ln\left(\frac{a_{Ox}}{a_{red}}\right) \quad (13)$$

where E^0 is the potential under standard conditions (V), R is the ideal gas law constant (8.314 J mol^{-1} K^{-1}), T is temperature (K), and a is the activity, which for a pure solid is unity, i.e., $a_M = 1$. From equation 13, the effect of increasing the concentration of oxidizing impurities (increasing a_{Ox}) leads to increasing E_c — thereby increasing ΔE_{rxn}, and results in a more negative ΔG_{rxn}. So far, the mathematical treatment around the Ellingham diagram is useful in predicting some experimental trends, such as the rate of depletion of certain alloying constituents. The diagram correctly predicts the rate of depletion for Mn > Cr > Fe > Ni [5, 11]. However, the diagram incorrectly predicts the rate of depletion of Nb, Mo, and W. Several studies have suggested the presence of these alloying constituents to slow down the rate of corrosion [10, 26].

Construction of chloride-oxide stability diagrams

The construction of a chloride-oxide stability diagram elucidates more information regarding the thermodynamic behavior of alloying constituents in molten chloride salts [10]. Such a diagram was constructed by calculating the ΔG_{rxn} of the oxides versus chlorides of various alloying constituents via HSC v8 (Fig. 2.).

Figure 2 has three primary regions:

i. Lower half representing oxide species are more stable than chloride species.

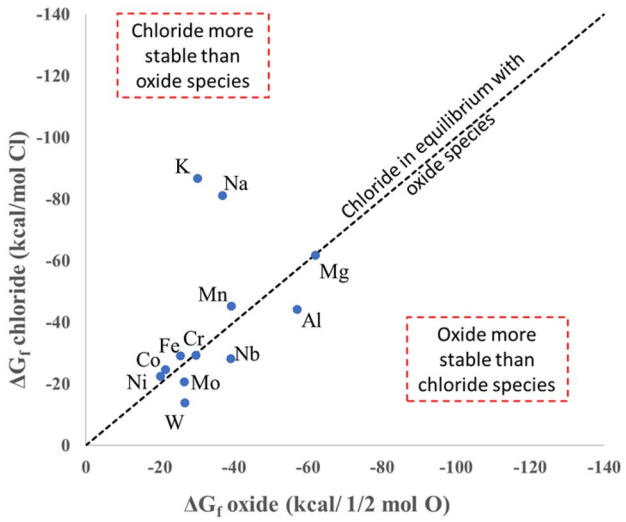

Fig. 2 Chloride-oxide stability diagram of various alloying constituents at 500°C

ii. Upper half representing chloride species are more stable than oxide species.
iii. Along the parity line, representing both oxide and chloride species in equilibrium with each other.

Several experimental observations can be explained via the chloride-oxide stability diagram. For example, K and Na chlorides are highly resistant to oxidation and can be considered stable in the presence of oxygen and moisture, whereas Mg is not [25]. Additionally, upon oxidation of Mn, Cr, Fe, Co, and Ni, the oxide will equilibrate with chloride ions and form chlorides as suggested by the chlorine-oxidation cycle. Lastly, alloys containing W, Mo, Al and Nb have enhanced corrosion resistance due to the formation of a relatively stable oxide that can serve as a passivation layer [10]. The utility of the chloride-oxide stability diagram elucidates several experimental observations that the typical Ellingham diagram overlooks. The diagram highlights that even Ni itself falls victim to the chlorine-oxidation cycle, as was observed by Liu et al. [5]. Even commercially pure Ni (e.g. Ni-201), which is expected to provide superior corrosion resistance, has been observed to corrode in chloride salt to a point of failure within days [26].

Combined use of Ellingham diagrams and chloride-oxide stability diagrams as predictive tools

Chloride-oxide stability diagrams and Ellingham diagrams are useful tools in evaluating corrosion and interpreting results, even in less well studied systems such as convective molten chloride systems. Though studies under these conditions are limited, notable examples include forced convection studies dating back to 1960s at the Brookhaven National Laboratory [12] and natural convection studies that were conducted in early 2010 between Idaho National Laboratory and the University of Wisconsin Madison [26]. We find that these examples are well explained by Chloride-oxide stability diagrams and Ellingham diagrams.

Natural convection corrosion studies elucidated time-dependent corrosion mechanisms [26, 27]. In the initial stages, corrosion is primarily driven by oxidative impurities, which can be understood using chloride-oxide stability analysis. Once the concentration of these impurities diminished, the corrosion was dominated by active dissolution of selective alloying constituents (e.g., Cr) from the hot side, and deposited on the cold site. The studies highlighted the effect of temperature-dependent metal solubilities of species such as chromium chloride. Similar observations were observed in the static corrosion study conducted by Gong et al. [20]. Under static conditions, the first 250 hours was primarily impurity-driven corrosion, after which the dominant mechanism became thermal effects resulting in metal solubility differences.

Surprisingly, forced convection corrosion studies conducted at Brookhaven National Laboratory observed no appreciable change in corrosion rates compared to static conditions [12]. The work highlighted the importance of salt purification and designing a leak tight system with an inert atmosphere. Therefore, an effective purification strategy can minimize corrosion by limiting the impurity-driven corrosion mechanism.

Conclusion

Corrosion remains a significant problem in molten chloride salts systems, but we propose that corrosion behavior of specific alloys can be predicted, and that experimental corrosion evaluation results can be understood, using a combination of Ellingham diagrams and chloride-oxide stability analysis. This method correlates corrosion behavior to fundamental thermodynamics and can be used to identify and explain performance of specific promising alloying elements. Thus, it can be used to identify high-performance alloys and to guide materials development toward appropriate alloys for use in molten chloride salts, which could in turn enable advances in chloride salt based CSP, nuclear, thermal energy storage, and other applications.

Acknowledgments The views expressed in the article do not necessarily represent the views of the DOE or the U.S. Government or any agency thereof. Neither the United States Government nor any agency thereof, nor any of their employees, makes any warranty, expressed or implied, or assumes any legal liability or responsibility for the accuracy, completeness, or usefulness of any information, apparatus, product, or process disclosed, or represents that its use would not infringe

Funding Open access funding provided by National Renewable Energy Laboratory Library. This work was authored in part by the National Renewable Energy Laboratory, operated by Alliance for Sustainable Energy, LLC, for the U.S. Department of Energy (DOE) under Contract No. DE-AC36–08GO28308. Funding provided by U.S. Department of Energy Office of Energy Efficiency and Renewable Energy Solar Energy Technologies Office grant CSP #35931 as well as the Colorado School of Mines/NREL Advanced Energy Systems Graduate Program. The views expressed in the article do not necessarily represent the views of the DOE or the U.S. Government. The U.S. Government retains and the publisher, by accepting the article for publication, acknowledges that the U.S. Government retains a nonexclusive, paid-up, irrevocable, worldwide license to publish or reproduce the published form of this work, or allow others to do so, for U.S. Government purposes.

Data Availability The authors confirm that the data supporting the findings of this study are available within the article.

Declarations

Conflict of interest On behalf of all authors, the corresponding author states that there is no conflict of interest.

References

1. M. Lambrecht, M.T. de Miguel, M.I. Lasanta, F.J. P'erez, Past research and future strategies for molten chlorides application in concentrated solar power technology. Solar Energy Mater. Solar Cells (2022). https://doi.org/10.1016/j.solmat.2021.111557
2. K. Vignarooban, X. Xu, A. Arvay, K. Hsu, A.M. Kannan, Heat transfer fluids for concentrating solar power systems - a review. Appl. Energy **146**, 383–396 (2015). https://doi.org/10.1016/j.apenergy.2015.01.125
3. W. Ding, A. Bonk, T. Bauer, Corrosion behavior of metallic alloys in molten chloride salts for thermal energy storage in concentrated solar power plants: a review. Front. Chem. Sci. Eng. **12**, 564–576 (2018). https://doi.org/10.1007/s11705-018-1720-0
4. B. Liu, X. Wei, W. Wang, J. Lu, J. Ding, Corrosion behavior of ni-based alloys in molten nacl-cacl2- $MgCl_2$ eutectic salt for concentrating solar power. Solar Energy Mater. Solar Cells **170**, 77–86 (2017). https://doi.org/10.1016/j.solmat.2017.05.050
5. M. Hofmeister, L. Klein, H. Miran, R. Rettig, S. Virtanen, R.F. Singer, Corrosion behaviour of stainless steels and a single crystal superalloy in a ternary LiCl-KCl-CsCl molten salt. Corros. Sci. **90**, 46–53 (2015). https://doi.org/10.1016/j.corsci.2014.09.009
6. K. Summers, D. Chidambaram, Corrosion in molten salts for solar thermal power. Electrochem. Soc. Interface (2021). https://doi.org/10.1149/2.F09212IF
7. S. Guo, J. Zhang, W. Wu, W. Zhou, Corrosion in the molten fluoride and chloride salts and materials development for nuclear applications. Prog. Mater. Sci. **97**, 448–487 (2018). https://doi.org/10.1016/j.pmatsci.2018.05.003
8. A.M. Kruizenga. Corrosion mechanisms in chloride and carbonate salts. Technical report, Sandia National Laboratory, 2012.
9. J.C. Gomez-Vidal, R. Tirawat, Corrosion of alloys in a chloride molten salt (nacl-licl) for solar thermal technologies. Solar Energy Mater. Solar Cells **157**, 234–244 (2016). https://doi.org/10.1016/j.solmat.2016.05.052
10. H. Susskind, F.B. Hill, L. Green, S. Kalish, L.E. Kukacka, W.E. McNulty, and E. Wirsing Jr. Corrosion studies for a fused salt-liquid metal extraction process for the liquid metal fuel reactor. Technical report, Brookhaven National Laboratory, 1960.
11. S. Choi, A.R. Strianese, O. Dale, M.F. Simpson, Electrochemical measurements for assessing corrosion of metal alloys in molten lif-naf-kf and $MgCl_2$-NaCl-Kcl. JOM **73**, 3544–3554 (2021). https://doi.org/10.1007/s11837-021-04843-3
12. J.M. Kurley, P.W. Halstenberg, A. McAlister, S. Raiman, S. Dai, R.T. Mayes, Enabling chloride salts for thermal energy storage: Implications of salt purity. RSC Adv. **9**, 25602–25608 (2019). https://doi.org/10.1039/c9ra03133b
13. C. Villada, W. Ding, A. Bonk, T. Bauer, Engineering molten $MgCl_2$–Kcl–NaCl salt for high-temperature thermal energy storage: review on salt properties and corrosion control strategies. Sol. Energy Mater. Sol. Cells **232**, 10 (2021). https://doi.org/10.1016/j.solmat.2021.111344
14. A. Mortazavi, Y. Zhao, M. Esmaily, A. Allanore, J. Vidal, N. Birbilis, High-temperature corrosion of a nickel-based alloy in a molten chloride environment – the effect of thermal and chemical purifications. Sol. Energy Mater. Sol. Cells **236**, 3 (2022). https://doi.org/10.1016/j.solmat.2021.111542
15. W. Ding, H. Shi, Y. Xiu, A. Bonk, A. Weisenburger, A. Jianu, T. Bauer, Hot corrosion behavior of commercial alloys in thermal energy storage material of molten $MgCl_2$/Kcl/NaCl under inert atmosphere. Solar Energy Mater. Solar Cells **184**, 22–30 (2018). https://doi.org/10.1016/j.solmat.2018.04.025
16. B. D'Souza, W. Zhuo, Q. Yang, A. Leong, J. Zhang, Impurity driven corrosion behavior of Haynes® 230® alloy in molten chloride salt. Corros. Sci. **187**, 7 (2021). https://doi.org/10.1016/j.corsci.2021.109483
17. X. Li, W. Liu, Z. Tang, Xu. Tingrui, J. Wang, Insight into dynamic interaction of molten $MgCl_2$-KCl-NaCl with impurity water via fpmd simulations. J. Mol. Liq. **314**, 9 (2020). https://doi.org/10.1016/j.molliq.2020.113596
18. M. Anderson and P. Sabharwall. Liquid salt heat exchanger technology for VHTR based applications: Reactor concepts rdd. Technical report, University of Wisconsin - Madison, 2012.
19. Q. Gong, H. Shi, Y. Chai, Yu. Rui, A. Weisenburger, D. Wang, A. Bonk, T. Bauer, W. Ding, Molten chloride salt technology for next-generation csp plants: compatibility of Fe-based alloys with purified molten $MgCl_2$-KCl-NaCl salt at 700 °C. Appl. Energy **324**, 10 (2022). https://doi.org/10.1016/j.apenergy.2022.119708
20. X. Song, G. Zhang, H. Tan, L. Chang, L. Cai, G. Xu, Z. Deng, Z. Han, Review on thermophysical properties and corrosion performance of molten salt in high temperature thermal energy storage. IOP Conf. Ser.: Earth Environ. Sci. **474**, 5 (2020). https://doi.org/10.1088/1755-1315/474/5/052071

21. K. Vignarooban, X. Xu, K. Wang, E.E. Molina, P. Li, D. Gervasio, A.M. Kannan, Vapor pressure and corrosivity of ternary metal-chloride molten-salt based heat transfer fluids for use in concentrating solar power systems. Appl. Energy **159**, 206–213 (2015). https://doi.org/10.1016/j.apenergy.2015.08.131
22. A.M. Gray. Corrosion mitigation of nickel alloy metals in molten chloride salts, 2021.
23. M. Taube. Fast reactors using molten chloride salts as fuel. Technical report, Federal Institute for Reactor Research, 1977.
24. Y. Zhao, N. Klammer, J. Vidal, Purification strategy and effect of impurities on corrosivity of dehydrated carnallite for thermal solar applications. RSC Adv. **9**, 41664–41671 (2019). https://doi.org/10.1039/c9ra09352d
25. W. Ding, A. Bonk, and T. Bauer. Molten chloride salts for next generation csp plants: Selection of promising chloride salts study on corrosion of alloys in molten chloride salts. Volume 2126. American Institute of Physics Inc., 7 2019. ISBN 9780735418660. https://doi.org/10.1063/1.5117729
26. E. Ogren, Thesis, University of Wisconsin, 2021
27. S.S. Raiman, S. Lee, Aggregation and data analysis of corrosion studies in molten chloride and fluoride salts. J. Nucl. Mater. **511**, 523–535 (2018). https://doi.org/10.1016/j.jnucmat.2018.07.036